Engineering Analysis with Boundary Elements ∎ (∎∎∎∎) ∎∎∎–∎∎∎

Contents lists available at ScienceDirect

Engineering Analysis with Boundary Elements

journal homepage: www.elsevier.com/locate/enganabound

Simulation of macrosegregation with mesosegregates in binary metallic casts by a meshless method

G. Kosec [a,b], B. Šarler [b,c,d,*]

[a] Jožef Stefan Institute, Department of Communication Systems, Jamova 39, 1000 Ljubljana, Slovenia
[b] University of Nova Gorica, Laboratory for Multiphase Processes, Vipavska 13, 5000 Nova Gorica, Slovenia
[c] Institute of Metals and Technology, Laboratory for Simulation of Materials and Processes, Lepi pot 11, 1000 Ljubljana, Slovenia
[d] Department of Information and Computing Sciences, School of Mathematics, Taiyuan University of Technology, Taiyuan, Shanxi Province, China

ARTICLE INFO

Article history:
Received 13 May 2012
Accepted 20 November 2013

Keywords:
Solidification
Macrosegregation
Mesosegragation
Instabilities
Meshless method
Local radial basis function collocation method
Local pressure corrections
Adaptive upwinding

ABSTRACT

Simulation of macrosegregation with mesosegregates as a consequence of solidification of a binary Sn–10%Pb alloy in a 2-dimensional rectangular cast is tackled in the present paper. Coupled volume averaged governing equations for mass, energy, momentum and species transfer are considered by incorporating Lever solidification rule and incompressible Newtonian fluid with Darcy limit in the mushy zone. Solid phase is assumed stationary. Double diffusive effects in the melt are modeled by the thermal and solutal Boussinesq hypothesis. The physical model is solved by the meshless Local Radial Basis Function Collocation Method (LRBFCM) by using 5-noded influence domains, multiquadrics radial basis functions and explicit time stepping. Pressure–velocity coupling is based on local pressure correction. Adaptive upwinding has to be used for stabilization of the convective terms. The numerical simulations reveal instabilities during solidification process that introduce anomalies in the final segregation map that scale with the typical cast as well as sub-cast dimensions. The main advantages of choosing the represented meshless approach for solving the problem are in its simplicity and similar coding in 2D and 3D, as well as straightforward applicability in non-uniform node arrangements. The locality of the proposed numerical approach is also convenient for parallel execution. It is demonstrated that LRBFCM can be advantageously used in casting simulations where the chemical segregation exhibits industrially relevant multi-scale patterns.

1. Introduction

Solidification science and engineering represents an interdisciplinary research field of great interest [1–4]. It is founded on thermodynamics and continuum mechanics that has to cope with solids and fluids simultaneously. Its analytical basis can be traced back to Lamé, Clapeyron, Neumann and Stefan [5], while the numerical treatment started by Douglas and Gallie in 1955 [6]. The solidification phenomena include nucleation, dendritic growth, eutectics, peritectics and microstructure selection issues, microsegregation, homogenization, and macro, meso and microstructures. Many modern industrial processes, in particular, different types of casting [7] rely on findings of solidification science and engineering. Castings are prone to several types of defects, such as porosities, deformation during solidification, including hot tearing, and chemical inhomogeneities also referred to as segregation. The segregation that scales with the whole casting is called macrosegregation, on the other hand, the segregation, much smaller than the size of the casting and much larger than the typical grain size is called mesosegregation. The theoretical description of the chemical segregation in solidification started in the Sixties [8], followed by more precise model studies in the Seventies [8,9]. Recently, this topic has been treated in many applied works, e.g. for static casting [10], continuous casting of steel [11] and direct chill casting of aluminum alloys [12]. Besides the applications, the physical modeling of the problem is also developing [13–16]. Solidification systems are difficult to treat in a closed form and actually only a few analytical solutions exist in connection with the subject [17–19]. Therefore, the use of numerical modeling and simulation is the preferred approach. The performance of numerical methods for solution of the macrosegregation problems remains rather unexplored. Recently, substantial efforts and resources were invested to study the behavior of different numerical methods in the prediction of macrosegregation [4,20], triggered in the framework of the French SMACS project, where a call for contributions to two numerical benchmark test cases was launched [21]. The test is gradually complicated from

* Corresponding author.
E-mail addresses: gkosec@ijs.si (G. Kosec), bozidar.sarler@ung.si (B. Šarler).

http://dx.doi.org/10.1016/j.enganabound.2014.01.016
0955-7997

Please cite this article as: Kosec G, Šarler B. Simulation of macrosegregation with mesosegregates in binary metallic casts by a meshless method. Eng. Anal. Boundary Elem. (2014), http://dx.doi.org/10.1016/j.enganabound.2014.01.016

natural convection of a low Prandtl fluid [22], double diffusive natural convection and to solidification of a binary material. In this work we present a solution of a third part of these benchmark tests by a novel meshless technique. The test deals with the solidification of a Sn–10%Pb alloy and follows our recent successful application of the same meshless technique for the first part of the benchmark [22]. The main complexities in numerical solution of alloy solidification models are moving interfaces with high gradients of physical properties, strong couplings between the conservation equations, different flow regimes in mushy zone and pure liquid, potentially unstable flow patterns in low-Pr liquids such as metals, hyperbolic nature of the solute transport due to almost completely advective transport. The problem of strong coupling between the momentum transport and energy and solute transport via the buoyancy force, and between the thermal field and permeability, makes the solution even more complex and less stable. The complexity of the prediction of macrosegregation is a consequence of the fact that the macrosegregation results from the entire history of the strongly coupled processes of mass, heat, momentum and solute transport from the liquid state up to the end of solidification. The channels (mesosegregates) in segregation profiles have been experimentally observed in different solidified products. In 1988 Sarazin and Hellawell performed analysis of channel formation in the directional solidification of the Pb–Sn alloys [23]. The experimental results, similar to the benchmark problem have been reported also in [24]. In this paper we focus on a numerical simulation of the phenomena with an emphasis on the meshless numerical technique.

The meshless or sometimes also named meshfree or mesh reduction methods represent a class of numerical methods where an arbitrarily distributed set of nodes, without any additional topological relations between them, is used. Such meshless methods represent a promising technique to avoid problems with polygonisation. There exist several meshless methods such as the Element free Galerkin method, the Meshless Petrov–Galerkin method, the point interpolation method, the point assembly method, the finite point method, smoothed particle hydrodynamics method, reproducing kernel particle method, and Kansa method [25–35]. This work is focused on one of the simplest classes of meshless methods in development today, the local point interpolation [36] Radial Basis Function [37] Collocation Method (RBFCM) [38]. In the present paper we use a local variant of RBFCM [38], the Local Radial Basis Function Collocation Method (LRBFCM). The main advantage of the local approach is that the spatial discretization of the problem is simplified to solving only small systems of algebraic equations instead of a large global system as in Kansa method [25,31] that might become unstable for increased number of computational nodes. The LRBFCM approach was already successfully applied to several thermo-fluid situations, ranging from laminar to turbulent as well as from single to two phase situations [39–44]. The LRBFCM has been recently also compared with GRBFCM and extended to the three dimensional problems [45–47].

2. Governing equations

The minimal solidification model, i.e. solidification model, simplified to the largest possible degree, is addressed in the present paper. The set of governing equations is based on continuum conservation laws and related constitutive relations. The model comprises energy transport, solute transport, incompressible Newtonian and porous Darcy fluid flow, and Eutectic phase diagram coupled with the solute transport over the phase front for consideration of the microscopic level. The model originates in the paper of Ni and Beckerman [13] and was later employed in many works [14–16]. In this paper we address the solidification in a two dimensional rectangular domain Ω with boundary Γ. The identical problem has been proposed in [21] within a call for a benchmark solutions. The problem is formulated as a system of four coupled Partial Differential Equations (PDE), Kozeny–Carman relation, Boussinesq approximation, and transport over the phase front on the microscopic scale, coupled with a phase diagram.

$$\nabla \cdot \mathbf{v} = 0, \tag{1}$$

$$\rho\frac{\partial \mathbf{v}}{\partial t} + \frac{\rho}{f_L}(\nabla \mathbf{v})\mathbf{v} = -f_L \nabla P + \mu \nabla^2 \mathbf{v} - f_L \frac{\mu}{K}\mathbf{v} + f_L \mathbf{b}, \tag{2}$$

$$\rho\frac{\partial h}{\partial t} + \rho \mathbf{v} \cdot \nabla h = \lambda \nabla^2 T, \tag{3}$$

$$\frac{\partial C}{\partial t} + \mathbf{v} \cdot \nabla C_L = 0 \tag{4}$$

$$\mathbf{v} = f_L \mathbf{v}_L, \tag{5}$$

$$K = K_0 \frac{f_L^3}{(1-f_L)^2}, \tag{6}$$

$$\mathbf{b} = \rho_{\mathrm{ref}}[1 - \beta_T(T - T_{\mathrm{ref}}) - \beta_C(C_L - C_{\mathrm{ref}})]\mathbf{g}, \tag{7}$$

$$h = c_p T + f_L L, \tag{8}$$

$$C = [f_L + (1-f_L)k_p]C_L, \tag{9}$$

$$T = T_F + m_L C_L \cdot \tag{10}$$

The following quantities are involved in the PDE: liquid velocity $\mathbf{v}$, intrinsic liquid velocity $\mathbf{v}_L$, enthalpy h, average concentration C, and the pressure P. The permeability K is defined through a permeability constant K_0 and the liquid fraction f_L. The thermophysical properties, i.e. viscosity μ, thermal conductivity λ, specific heat c_p and density ρ are assumed to be equal and constant in both phases. The buoyancy term $\mathbf{b}$ depends on the temperature T, the liquid concentration C_L, the thermal expansion coefficient β_T, the concentration expansion coefficient β_C, the reference density ρ_{ref} given at the reference temperature T_{ref} and the reference concentration C_{ref}. The binary phase diagram is defined by the liquidus slope m_L, the equilibrium partition coefficient k_p and fusion temperature of the pure solvent T_F. Symbols t and $\mathbf{g}$ stand for time and gravity acceleration, respectively. We seek the solution of the temperature, velocity, pressure and concentration fields at time $t = t_0 + \Delta t$, where t_0 represents initial time and Δt a positive time increment. The problem is schematically presented in Fig. 1. In [48] it was shown that the presented "minimal" solidification model can be solved with the presented local meshless based solution procedure for cases without mesosegregate anomalies. In the present paper we present a solution of the SMACS benchmark solidification exercise for the alloy Sn–10%Pb (see Table 1 for thermo-physical properties). This case is from the numerical point of view considerably more difficult to solve due to the presence of mesosegregates. The case is defined for a rectangular domain with dimensions 10×6 cm. However, computational domain can be reduced to 5×6 cm due to the symmetry (Fig. 1).

The initial and boundary conditions are set to

$$\mathbf{v}(p_x = \Omega_W, t) = \mathbf{v}(p_y = \Omega_H, t) = \mathbf{v}(p_y = 0, t) = 0, \tag{11}$$

$$\frac{\partial}{\partial p_x} v_y(p_x = 0,\ t) = 0,\ v_x(p_x = 0,\ t) = 0, \tag{12}$$

$$\frac{\partial}{\partial p_x} T(p_x = \Omega_W, t) = \frac{q}{\lambda}(T - T_{ext}) \tag{13}$$

$$\frac{\partial}{\partial p_x} T(p_x = 0, t) = \frac{\partial}{\partial p_y} T(p_y = 0, t) = \frac{\partial}{\partial p_y} T(p_y = \Omega_H, t) = 0 \tag{14}$$

Please cite this article as: Kosec G, Šarler B. Simulation of macrosegregation with mesosegregates in binary metallic casts by a meshless method. Eng. Anal. Boundary Elem. (2014), http://dx.doi.org/10.1016/j.enganabound.2014.01.016

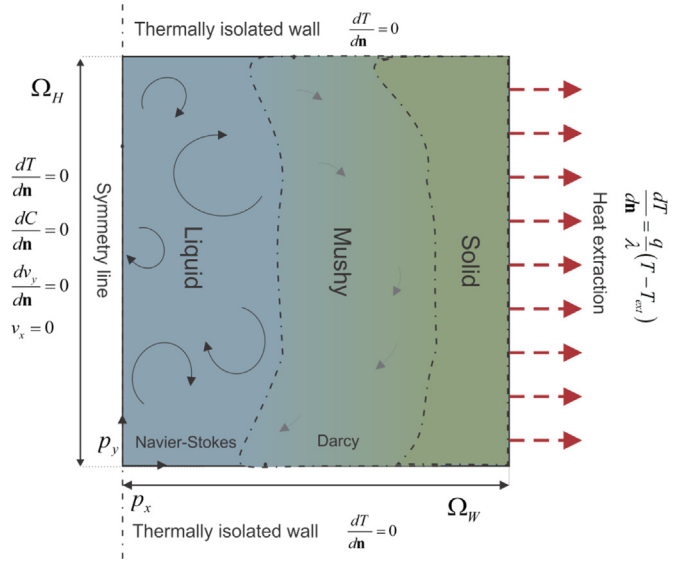

Fig. 1. The setup of solidification benchmark test.

Table 1
Thermo-physical properties and process parameters.

Property	symbol	Sn–10%Pb	Pb–18%Sn	Units
Density	ρ	7.00e+03	9.25e+03	kg/m^3
Specific heat	c_p	2.60e+02	1.76e+02	J/kgK
Thermal conductivity	λ	5.50e+01	1.79e+01	W/mK
Latent heat of fusion	L	6.10e+04	3.76e+04	J/kg
Liquid dynamic viscosity	μ	1.00e−03	1.10e−03	Pa s
Thermal expansion coefficient	β_T	6.00e−05	1.16e−04	K^{-1}
Solutal expansion coefficient	β_C	−5.30e−03	4.90e−03	%-1
Reference temperature	T_{ref}	2.20e+02	2.85e+02	°C
Reference concentration	C_{ref}	1.00e+01	1.80e+01	%
Reference density	ρ_{ref}	7.00e+03	9.25e+03	kg/m^3
Permeability constant	K_0	2.34e−11	1.90e−10	m^2
Melting temperature	T_f	2.32e+02	3.27e+02	°C
eutectic temperature	T_e	1.83e+02	1.83e+02	°C
eutectic concentration	C_e	3.81e+01	6.19e+01	%
Solubility at eutectic temperature	C_{eS}	2.49e+00	1.92e+01	%
Liquidus slope	m_L	−1.28e+00	−2.33e+00	°C/%
Gravity acceleration $\mathbf{g}=g_y\mathbf{i}_y$	g_y	−9.80e+00	−9.80e+00	m/s^2
External temperature	T_{ext}	25	25	°C
Heat transfer coefficient	q	400	400	W/m^{2}K

$$\frac{\partial}{\partial p_x}C(p_x=0,t)=0, \tag{15}$$

$$C(p_x=\Omega_W,\ t)=C(p_y=\Omega_H,\ t)=C(p_y=0,\ t)=C_0, \tag{16}$$

$$\mathbf{v}(\mathbf{p},\ t=0)=0,\ T(\mathbf{p},t=0)=T_0,\ C(\mathbf{p},t=0)=C_0, \tag{17}$$

where Ω_H and Ω_W stand for the rectangle height and width, respectively. The case is schematically presented in Fig. 1.

3. Local meshless solution procedure

The main challenge that we address in this paper is solution of a non-linear and strongly coupled system of partial differential equations (PDE). The spatial discretization of the governing PDE is performed by a relatively new, but well tested local meshless numerical approach. The mass and momentum conservation coupling, essential in fluid mechanics, is done by a local coupling. The complete locality of the numerical scheme has several beneficial effects. Besides simplicity and straightforward numerical implementation is the approach suitable to fully exploit modern computer architectures through different parallel computing strategies [34]. It is important to point out that the typical solidification simulations require vast amount of computational resources; hence the efficiency of computer implementation is of major importance. The details of LRBFCM can be perceived from [39,48,49]. We elaborate the important basics of the method, particularly the adaptive upwinding and pressure–velocity coupling in the continuation of the present paper. The LRBFCM spatial discretization is based on an approximation of a considered field over the support domain with trial functions. The radial basis functions are used for trial functions and their coefficients are determined by collocation. The locality of the method is introduced in the selection of a local support domain, i.e. only local sub-clusters of nodes are considered in support domain. An approximated function $\theta(\mathbf{p})$, where $\mathbf{p}$ represents a position vector, is introduced as a sum of weighted basis functions

$$\theta(\mathbf{p})=\sum_{n=1}^{N_{Basis}}\alpha_n\Psi_n(\mathbf{p}), \tag{18}$$

where N_{Basis}, α_n and Ψ_n stand for the number of trial functions, the approximation coefficients and the trial functions, respectively. The approximation coefficients are obtained from collocation of Eq. (18) in points $\mathbf{p}_n; n=1,2,\ldots, N_{Basis}$ where the values of $\theta(\mathbf{p}_n)$ are known. In this paper we use Hardy's Multiquadrics (MQs) as trial functions

$$\Psi_n(\mathbf{p})=\sqrt{(\mathbf{p}-\mathbf{p}^n)\cdot(\mathbf{p}-\mathbf{p}^n)/\sigma_C^2+1}, \tag{19}$$

where σ_C stands for the free shape parameter. With the constructed collocation function, action of an arbitrary spatial differential operator L can be computed

$$L\theta(\mathbf{p})=\sum_{n=1}^{N_{Basis}}\alpha_n L\Psi_n(\mathbf{p}) \tag{20}$$

The implementation of the Dirichlet boundary condition is straightforward. In order to implement Neumann and Robin boundary conditions a special case of interpolation is needed. In these boundary nodes the function directional derivative instead of the function value is known and therefore the equation in the interpolation system changes to

$$\theta_{BC}=\sum_{n=1}^{N_{Basis}}\alpha_n\left(a\frac{\partial}{\partial\mathbf{n}}\Psi_n(\mathbf{p})+b\Psi_n(\mathbf{p})\right), \tag{21}$$

where a and b define considered boundary condition.

The well-known upwind stabilization technique, originally developed in connection with FDM by Courant [50], is being used to treat the completely advective solute transport. To minimize the numerical dissipation, the upwind offset is derived from the local field values and configuration of the influence domain. The proposed adaptive upwind scheme [51] uses local Péclét number to evaluate magnitude and direction of the upwind offset ($\boldsymbol{\delta}$) (Fig. 2).

$$\boldsymbol{\delta}=\frac{\mathbf{v}}{||\mathbf{v}||}\left[\text{cth}(\text{Pe})-\frac{1}{\text{Pe}}\right]p^{NRM}\sigma_{UW}, \tag{22}$$

where σ_{UW} is a parameter determining the maximum offset normalized to the characteristic influence domain (p^{NRM}). In the present case p^{NRM} is set to the maximal distance between the support domain nodes. The σ_{UW} is used to control the magnitude of upwind used. The described upwind has been already used in the context of LRBFCM in simulation of turbulent fluid flow [49]. In this work upwind is used for alleviating the instabilities of advection term in solute transport equation (4).

Please cite this article as: Kosec G, Šarler B. Simulation of macrosegregation with mesosegregates in binary metallic casts by a meshless method. Eng. Anal. Boundary Elem. (2014), http://dx.doi.org/10.1016/j.enganabound.2014.01.016

The temporal discretization is done through the use of two-level explicit time stepping

$$\rho_0\frac{\theta-\theta_0}{\Delta t}=\nabla\cdot(D_0\nabla\theta_0)-\nabla\cdot(\rho_0\mathbf{v}_0\theta_0)+S_0, \tag{23}$$

where zero-indexed quantities stand for the values at the initial time, and D, S for general diffusion coefficient, and source term, respectively. The time step is denoted with Δt. The pressure–velocity coupling is performed through the correction of the pressure, based on the divergence on the intermediate velocity ($\hat{\mathbf{v}}$), computed from discrete variant of Eq. (2).

$$\hat{P}^{m+1}=\hat{P}^m+\zeta\frac{\rho}{\Delta t}\frac{1}{f_L}\nabla\cdot\hat{\mathbf{v}}^m, \tag{24}$$

with index m bookkeeping the iteration. The corrected pressure is used to re-compute new intermediate velocity. The iterations take place until a reasonably solenoidal velocity field is achieved. The approach has been extensively tested in [22,42]. The represented coupling is similar to the artificial compressibility method (ACM) [52,53] or the SOLA approach [54]. However, the ACM and SOLA do not use internal iteration for velocity correction and as such do not assure precise transient solution.

The coupling between the conservation equations and the phase change is also determined locally. The use of Level rule for determination of the phase change simplifies the coupling to the

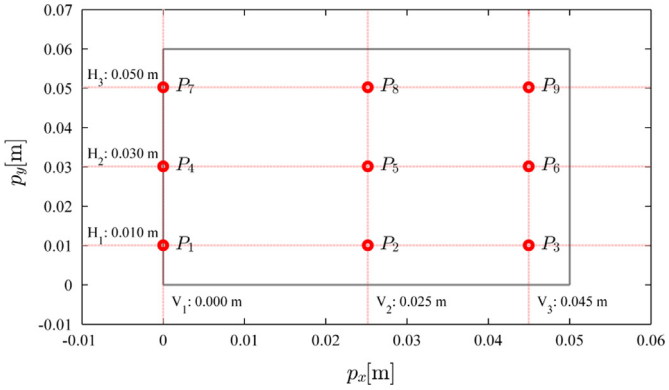

Fig. 3. Definition of benchmark control points and cross-section lines. *P* stands for control points, V for vertical and H for horizontal cross-section lines.

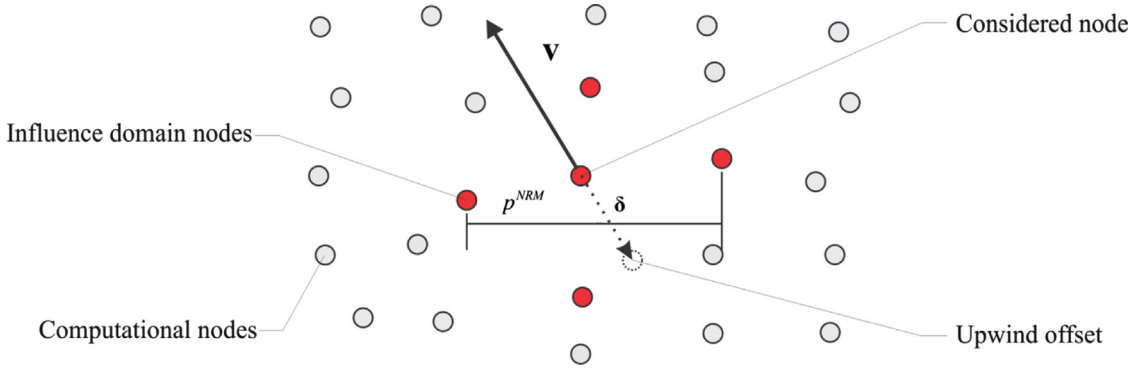

Fig. 2. Scheme of the upwind technique in the meshless context. The function value is calculated instead of in the considered node in the upwind offset position.

Table 2
Representation of the results in tabular form: values of main variables in control points throughout the solidification process.

Control point	t(S)	10	90	170	250	330	410	490	570
1	T(°C)	219.14	218.11	214.88	207.19	192.34	182.03	141.33	110.05
2		219.14	215.58	206.58	197.11	185.30	169.49	136.59	106.59
3		217.45	199.82	188.33	180.80	169.73	153.24	126.43	99.16
4		219.14	218.72	216.51	207.84	191.44	181.25	141.30	110.05
5		219.14	216.49	207.47	197.36	184.72	168.70	136.57	106.59
6		217.50	200.57	188.75	180.89	169.16	152.87	126.41	99.16
7		219.14	219.01	217.62	208.45	190.84	180.61	141.28	110.05
8		219.14	217.26	208.18	197.60	184.22	168.13	136.54	106.59
9		217.70	201.18	189.09	180.91	168.65	152.54	126.39	99.16
1	f_l	1.00	1.00	1.00	0.82	0.49	0.37	0.00	0.00
2		1.00	0.77	0.47	0.33	0.23	0.00	0.00	0.00
3		0.88	0.36	0.25	0.12	0.00	0.00	0.00	0.00
4		1.00	1.00	1.00	0.74	0.42	0.32	0.00	0.00
5		1.00	0.78	0.45	0.30	0.20	0.00	0.00	0.00
6		0.88	0.37	0.25	0.12	0.00	0.00	0.00	0.00
7		1.00	1.00	1.00	0.64	0.34	0.26	0.00	0.00
8		1.00	0.79	0.42	0.27	0.17	0.00	0.00	0.00
9		0.87	0.34	0.22	0.11	0.00	0.00	0.00	0.00
1	C(%)	10.00	10.97	13.31	16.10	16.09	16.09	16.09	16.09
2		10.00	9.98	10.02	10.03	10.02	10.02	10.02	10.02
3		10.01	10.05	10.05	10.05	10.05	10.05	10.05	10.05
4		10.00	10.29	12.04	14.29	14.30	14.30	14.30	14.30
5		10.00	9.61	9.32	9.24	9.24	9.24	9.24	9.24
6		9.99	9.95	9.94	9.94	9.94	9.94	9.94	9.94
7		10.00	10.09	11.19	12.16	12.16	12.16	12.16	12.16
8		10.00	9.22	8.50	8.40	8.40	8.40	8.40	8.40
9		9.79	9.14	9.08	9.08	9.08	9.08	9.08	9.08

Please cite this article as: Kosec G, Šarler B. Simulation of macrosegregation with mesosegregates in binary metallic casts by a meshless method. Eng. Anal. Boundary Elem. (2014), http://dx.doi.org/10.1016/j.enganabound.2014.01.016

following closed form solution [48]

$$\begin{aligned} &af_L^2+bf_L+c=0,\\ &a=(k_p-1)L,\\ &b=(k_p-1)(c_pT_F-h)-k_pL,\\ &c=k_p(h-c_pT_F)-c_pm_LC\cdot \end{aligned} \tag{25}$$

4. Numerical implementation

The presented numerical methodology is implemented in C++ programming language and compiled with Intel compiler 13. The numerical method, including the pressure velocity coupling, is completely local, therefore the bulk of the computationally demanding part of the code is parallelized through the OpenMP

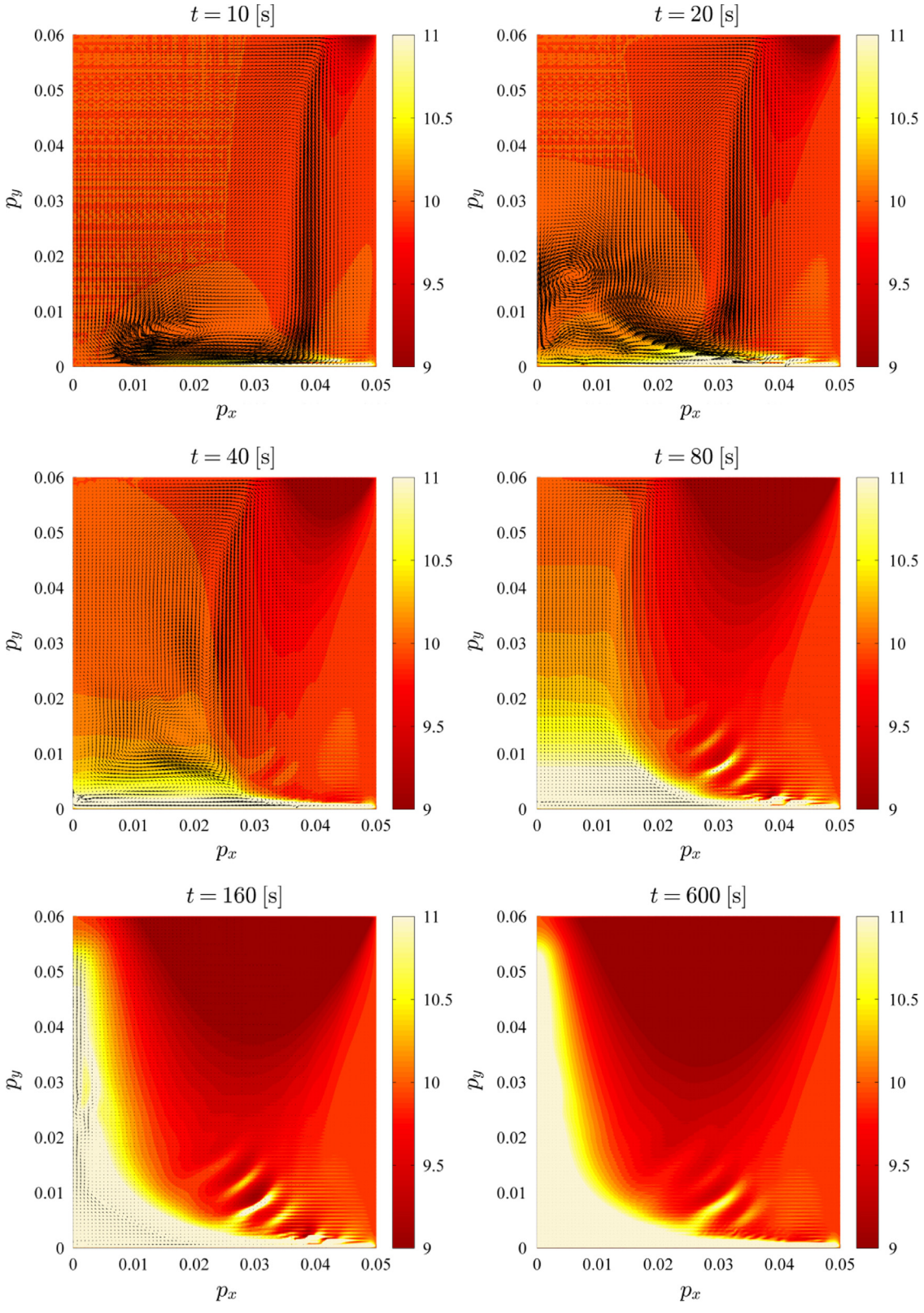

Fig. 4. Concentration and velocity at different stages of solidification. Last (bottom right) plot stands for fully solidified state.

API. All computations are done on CPU Intel(R) Xeon(R) E5520 @ 2.27 GHz based computers. A detailed execution performance of the presented numerical methodology, i.e. speedup analyses, cache utilization, etc, has been recently presented for a shared memory parallelization [55] and for multiple Graphics Processing Units [56].

In all computations five nodded support domains are used and the meshless shape parameter is set to $\sigma_C = 90$. All computations are done with time step $\Delta t = 10^{-5}$ and pressure–velocity relaxation parameter is set to $\zeta = 10^{-8}$.

5. Results and discussion

The solidification of Sn–10%Pb alloy is considered with the process parameters defined in Table 1. The solidification transient starts with a well-mixed ($C_o = 10\,\%$), stationary over-heated liquid ($T_0 = 220$ °C). The heat is extracted from the right side of the domain, described by the Robin boundary conditions. As the initial liquid cools, the thermo-solutal natural convection is set up.

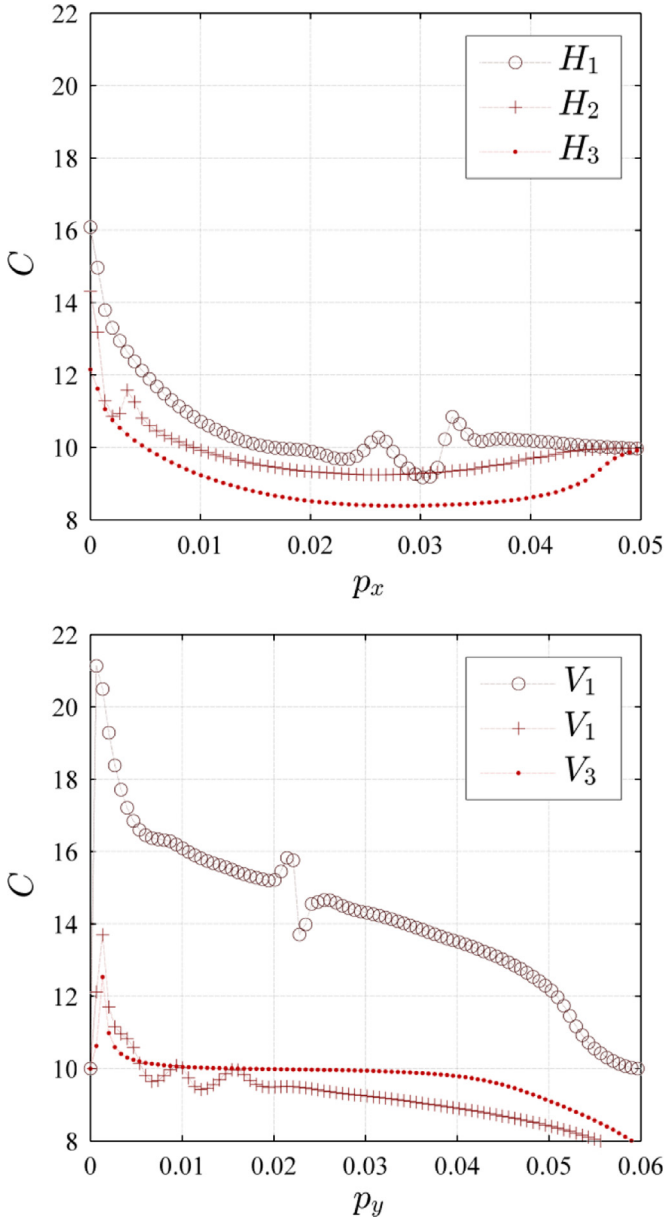

Fig. 5. Concentration horizontal (left) and vertical (right) cross-sections of the steady state concentration profile.

The thermal and solutal natural convection (7) drives the flow clockwise. The solidification process starts when the liquid temperature reaches the Liquidus temperature (Table 2). The main characteristics of the segregation are visible soon after the beginning of the solidification. The only mechanism for solute transport is the advection (4) thus the segregation characteristics, at least on a global scale, depends only on the main flow behavior. A positive segregation patch at the bottom of the enclosure and a negative segregation patch in the upper part is clearly visible. The pattern can be explained by combining Eq. (3) and Eq. (10) into

$$\frac{\partial C}{\partial t} = -\frac{1}{m_L}\mathbf{v}\cdot\nabla T \tag{26}$$

Eq. (26) shows the dependence of segregation tendency on the direction of the flow and the isotherms (note that $m_L < 0$). The isotherms are in both cases similar, therefore the macrosegregation

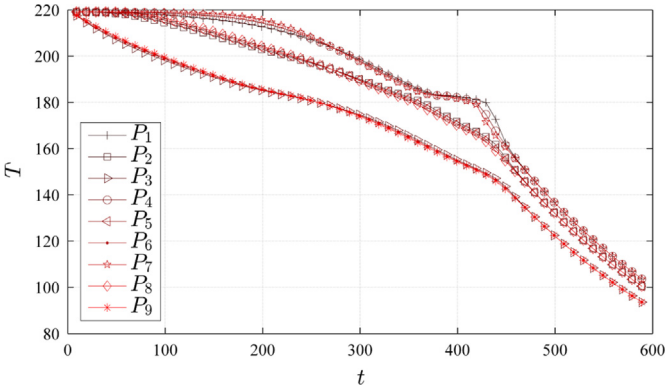

Fig. 6. Temporal development of temperature in control points.

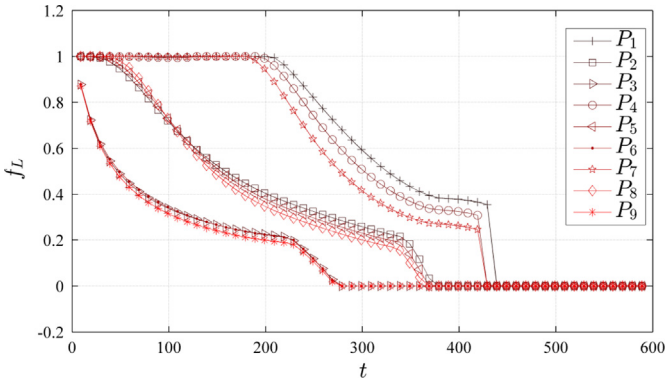

Fig. 7. Temporal development of liquid fraction in control points.

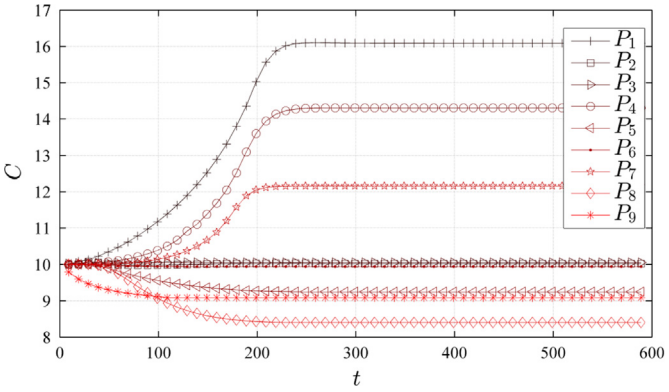

Fig. 8. Temporal development of concentration in control points.

Please cite this article as: Kosec G, Šarler B. Simulation of macrosegregation with mesosegregates in binary metallic casts by a meshless method. Eng. Anal. Boundary Elem. (2014), http://dx.doi.org/10.1016/j.enganabound.2014.01.016

profile is governed by the flow only. Besides the macrosegregation, the formation of mesosegrates starts in the mushy zone as the solidification front advances. The channel-like anomalies in concentration field occur as a consequence of instabilities in the porous mushy zone. The solidification in the channels is slowed down, i.e. the solid fraction in the channels is lower and consequently the hydrodynamic permeability is higher. The lower drag in the channels makes the flow through the channels stronger, and the stronger flow induces stronger segregation (26). The mechanisms of the initial destabilization are still unknown. It is not yet clear what generates the first perturbation. However, phenomenon has been observed experimentally [57], which confirms that such behavior is not a product of numerical instabilities but of a not yet explained natural phenomenon. After a first perturbation the strong couplings between transport mechanics and phase change amplify the effect until the material is completely solidified.

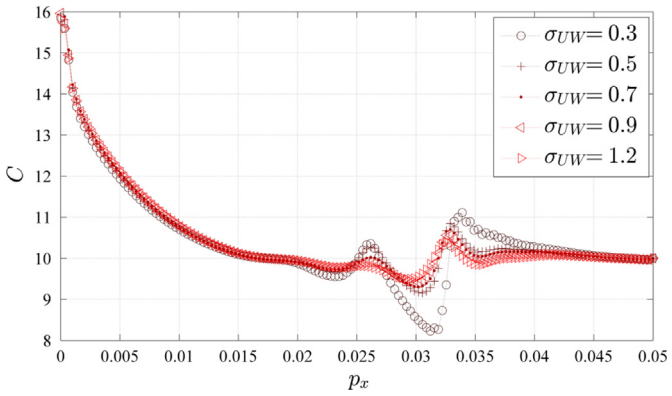

Fig. 9. Effect of the upwind magnitude on the simulation results. The concentration cross-sections at V_1 for different upwind magnitudes.

The solidification process is presented in Fig. 4, where the concentration profiles, together with the velocity fields, are plotted for different stages of the solidification. The results are computed with 27,000 uniformly distributed nodes and upwind magnitude $\sigma_{UW} = 0.5$. The results are further analyzed on cross-sections and control points defined in Fig. 3. In Fig. 5 horizontal and vertical cross-sections of steady-state concentration are presented. Furthermore, temporal developments of temperature (Fig. 6), liquid fraction (Fig. 7), and concentration (Fig. 8) are presented in nine control points. (P1-9). The adaptive upwind stabilization of the advection term is used to solve the problem. The magnitude of the stabilization should be minimal, since the upwind introduces artificial numerical diffusion. The analysis of the influence of the upwind magnitude is presented in Fig. 9. It can be clearly seen that a

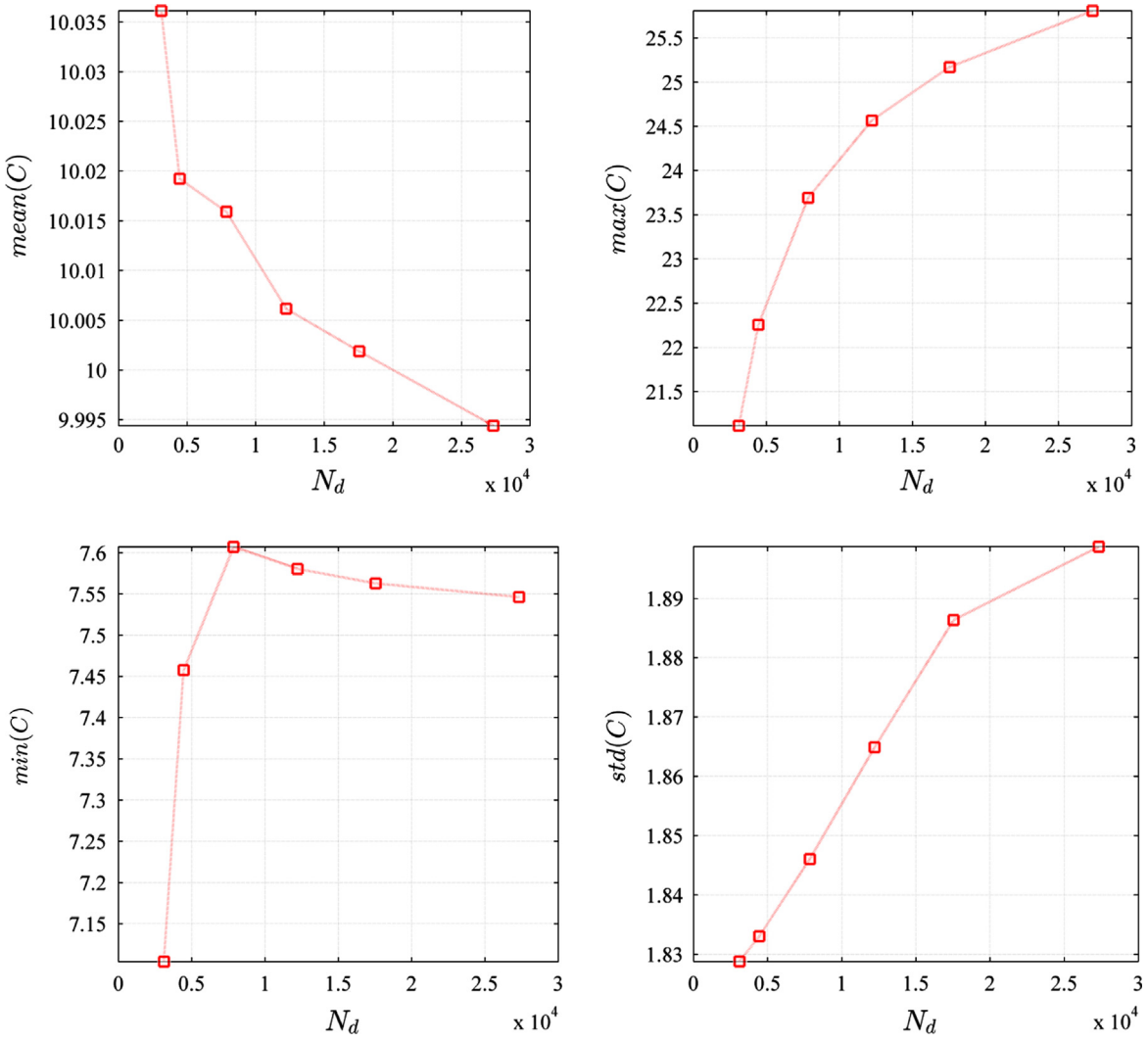

Fig. 10. Convergence plots as a function of the density of spatial discretization in terms of mean (top left), maximum (top right), and minimum (bottom left) value, and standard deviation (bottom right) of the steady state concentration.

Please cite this article as: Kosec G, Šarler B. Simulation of macrosegregation with mesosegregates in binary metallic casts by a meshless method. Eng. Anal. Boundary Elem. (2014), http://dx.doi.org/10.1016/j.enganabound.2014.01.016

stronger upwind diminishes the mesosegregation patterns, but when using too low upwind, the results diverge. Respectively, we use a reasonably small upwind magnitude ($\sigma_{UW} = 0.5$).

Finally, we present the convergence plot in terms of mean, max and min value, and standard deviation of steady state concentration profile in Fig. 10.

Five computer codes have been recently used to simulate a similar (Exercise 2 from in [4]) with mesosegregates, as tackled in the present paper. Four computer codes were based on the finite volume formulation and one code was based on the finite element method with unstructured triangular mesh. We can observe that even though the qualitative macrosegregation pattern with mesosegregates of the different solutions is the same, notable differences exist in the evolutions and local behavior. The main differences are located in the channels and in their vicinity. The number of channels and the intensity of segregation inside the channels vary from one computer code to another. Even with fine meshes, it has not been possible to find a unique solution, mesh independent and similar to all the contributions. See the details in [4]. Respectively, also the contribution in the present paper cannot be considered as fully converged, however we believe the best on the involved node density. The present paper shows that LRBFCM is capable of solving such complex problems. Furthermore, the local pressure–velocity coupling is successfully employed for computations of fluid-flow through the mushy zone in the presence of instabilities.

6. Conclusions

A physical model for calculating the macrosegregation with mesosegragates in the cast has been numerically solved in the present paper. The conditions correspond to the numerical Exercise 1 in [21]. By the best knowledge of the present authors no other published references exist with respect to the tackled case. Extensive tabulation of the results has been done respectively, in order to facilitate comparisons with alternative numerical approaches. The problem is highly nonlinear, since it includes

- completely advective transport of species that is unstable by its nature,
- potential unstable natural convection in the low-Prandtl liquids such as metals,
- the high jump in the enthalpy near the phase change,
- and the presence of two flow regimes; free fluid and Darcy porous media flow in the mushy zone.

The nonlinearities are combined with the following strong couplings:

- between the mass and momentum conservation,
- between the momentum transport and energy and solute transport via buoyancy force,
- between the thermal field, concentration field and permeability,
- between the permeability and fluid flow.

The LRBFCM is for the first time used to solve macrosegregation problems that exhibits mesosegregation as a consequence of the above listed physical features. We demonstrate that such complex problems can be tackled with the represented extremely straightforward and intuitive meshless numerical approach that needs to include adaptive upwind. We measure the effect of this stabilization tool on the results and show high sensitivity of the results on the selection of the upwind magnitude. The proposed novel meshless method shows several convenient properties like straightforward implementation and parallelization suitability, CPU effectiveness and several degrees of freedom for optimization, which makes the method flexible. The dynamic point adaptivity strategy [58,59] makes it a promising alternative even for complex problems of the same kind. This might replace the need for adaptive upwind. Related attempts are in the focus of our future research, together with coupling of the macro-mesoscopic predictions with the cellular automata based grain structure evolution. A compatible meshless strategy, relying on points instead of polygons has been developed recently [60].

Acknowledgment

We acknowledge the financial support from the Slovenian Research Agency under the grant J2-4120 and program group P2-0379.

References

[1] Flemings MC. Solidification Processing. Metall Mater Trans A 1974;B5:2121–34.
[2] Dantzig J, Rappaz M. Solidification. Laussane: EPFL Press; 2009.
[3] Kurz W, Fisher DJ. Fundamentals of solidification. Boca Raton: CRC Press; 1998.
[4] Combeau H, Bellet M, Fautrelle Y, Gobin D, Arquis E, Budenkova O, et al. Analysis of a numerical benchmark for columnar solidification of binary alloys. IOP Conf Ser Mater Sci Eng 2012;33:012086.
[5] Šarler B. Stefan's work on solid-liquid phase changes. Eng Anal Bound Elem 1995;16:83–92.
[6] Douglas J, Gallie TM. On the numerical integration of a parabolic differential equation subject to a moving boundary condition. Duke Math J 1955;22:557–71.
[7] Cockcroft LS, Maijer DM. Modeling of casting, welding, and advanced solidification processes XII. Warrendale: The Minerals, Metals & Materials Society; 2009.
[8] Flemings MC. Nereo GE. macrosegregation, part I. Trans Soc Metals AIME 1967;239:1449–61.
[9] Hebditch DJ, Hunt JD. Observations of ingot macrosegregation on model systems. Metall Trans 1974;5:1557–64.
[10] Založnik M, Kumar A, Combeau H. An operator splitting scheme for coupling macroscopic transport and grain growth in a two-phase multiscale solidification model: Part II application of the model. Comp Mater Sci 2010;48:11–21.
[11] Lesoult G. Macrosegregation in steel strands and ingots: characterisation, formation and consequences. Mat Sci Eng A-Struct 2005;413-414:19–29.
[12] Založnik M, Šarler B. Modeling of macrosegregation in direct-chill casting of aluminum alloys: estimating the influence of casting parameters. Mater Sci Eng 2005;A413-414:85–91.
[13] Ni J, Beckermann C. A volume-averaged two-phase model for transport phenomena during solidification. Metall Mater Trans A 1991;22B:349–61.
[14] Drew DA. Mathematical modeling of two-phase flow. Annu Rev Fluid Mech 1983;15:261–91.
[15] Wang CY, Beckermann C. Equiaxed dendritic solidification with convection: Part I. multiscale/multiphase modeling. Metall Mater Trans A 1996;A27:2754–64.
[16] Goyeau B, Bousquet-Melou P, Gobin D, Quintard M, Fichot F. Macroscopic modeling of columnar dendritic solidification. Comput Appl Math 2004;23:381–400.
[17] Voller VR, Mouchmov A, Cross M. An explicit scheme for coupling temperature and concentration fields in solidification models. Appl Math Model 2002;28:79–94.
[18] Voller VR. On a general back-diffusion parameter. J Cryst Growth 2001;226:562–8.
[19] Swaminathan C, Voller VR. Towards a general numerical scheme for solidification scheme. Int J Heat Mass Transfer 1996;40:2859–68.
[20] Combeau H, Bellet M, Fautrelle Y, Gobin D, Arquis E, Budenkova O, et al. A numerical benchmark on the prediction of macrosegregation in binary alloys. In: Proceedings of frontiers in solidification science. Warrendale, USA: TMS2011.
[21] Bellet M, Combeau H, Fautrelle Y, Gobin D, Rady M, Arquis E, et al. Call for contributions to a numerical benchmark problem for 2D columnar solidification of binary alloys. Int J Therm Sci 2009;48:2013–6.
[22] Kosec G, Šarler B. Solution of a low Prandtl number natural convection benchmark by a local meshless method. Int J Numer Method H 2013;23:22.
[23] Sarazin JR, Hellawell A. Channel formation in Pb-Sn, Pb-Sb, and Pb-Sn-Sb alloy ingots and comparison with the system NH4CI-H2O. Metall Trans 1988;19:1861–71.
[24] Quillet G, Ciobanas A, Lehmann P, Fautrelle Y. A benchmark solidification experiment on an Sn–10% wtBi alloy. Int J Heat Mass Transfer 2007;50:654–66.
[25] Kansa EJ. Multiquadrics - a scattered data approximation scheme with application to computational fluid dynamics, part I. Comput Math Appl 1990;19:127–45.
[26] Chen W. New RBF collocation schemes and kernel RBFs with applications. Lecture Notes in Computer Science 2002;26:75–86.

Please cite this article as: Kosec G, Šarler B. Simulation of macrosegregation with mesosegregates in binary metallic casts by a meshless method. Eng. Anal. Boundary Elem. (2014), http://dx.doi.org/10.1016/j.enganabound.2014.01.016

[27] Atluri SN, Shen S. The meshless local Petrov-Galerkin (MLPG) method: a simple & less-costly alternative to the finite element and boundary element methods. CMES-Comp Model Eng 2002;3:11–52.
[28] Liu GR. Mesh free methods. Boca Raton: CRC Press; 2003.
[29] Liu GR, Gu YT. An introduction to meshfree methods and their programming. Dordrecht: Springer; 2005.
[30] Atluri SN, Shen S. The meshless method. Encino: Tech Science Press; 2002.
[31] Kansa EJ. Multiquadrics - a scattered data approximation scheme with application to computational fluid dynamics, part II. Comput Math Appl 1990;19:147–61.
[32] Fasshauer G. Radial basis functions and related multivariate meshfree approximation methods: theory and applications – preface. Comput Math Appl 2006;51:1223–366.
[33] Monaghan JJ. An Introduction to SPH. Comput Phys Commun 1988;48:89–96.
[34] Trobec R, Šterk M, Robič B. Computational complexity and parallelization of the meshless local Petrov-Galerkin method. Comput Struct 2009;87:81–90.
[35] Šterk M, Trobec R. Meshless solution of a diffusion equation with parameter optimization and error analysis. Eng Anal Bound Elem 2008;32:567–77.
[36] Wang JG, Liu GR. A point interpolation meshless method based on radial basis functions. Int J Numer Meth Eng 2002;54:1623–48.
[37] Buhmann MD. Radial basis functions. Cambridge: Cambridge University Press; 2000.
[38] Šarler B. From global to local radial basis function collocation method for transport phenomena. Advances in meshfree techniques. Berlin: Springer; 2007; 257–82.
[39] Šarler B, Vertnik R. Meshfree explicit local radial basis function collocation method for diffusion problems. Comput Math Appl 2006;51:1269–82.
[40] Vertnik R, Šarler B. Meshless local radial basis function collocation method for convective-diffusive solid-liquid phase change problems. Int J Numer Method H 2006;16:617–40.
[41] Divo E, Kassab AJ. Localized meshless modeling of natural-convective viscous flows. Numer Heat Transfer 2007;B129:486–509.
[42] Kosec G, Šarler B. Solution of thermo-fluid problems by collocation with local pressure correction. Int J Numer Method H 2008;18:868–82.
[43] Mramor K, Vertnik R, Low Šarler B. and Intermediate Re solution of Lid driven cavity problem by local radial basis function collocation method. CMC-Comput Mater Con 2013;1:1–21.
[44] Kosec G, Šarler B. Solution of phase change problems by collocation with local pressure correction. CMES-Comp Model Eng 2009;47:191–216.
[45] Yao G, Šarler B. Assessment of global and local meshless methods based on collocation with radial basis functions for parabolic partial differential equations in three dimensions. Eng Anal Bound Elem 2012:36.
[46] Siraj Ul I, Vertnik R, Šarler B. Numerical solution of the two-dimensional transient nonlinear coupled burgers' equations. Appl Math Model 2012:36.
[47] Siraj Ul I, Šarler B, Vertnik R. Local radial basis function collocation method along with explicit time stepping for hyperbolic partial differential equations. Appl Numer Math 2013;67:136–51.
[48] Kosec G, Založnik M, Šarler B, Combeau H A. Meshless approach towards solution of macrosegregation phenomena. CMC-Comput Mater Con 2011;580:1–27.
[49] Vertnik R, Šarler B. Solution of incompressible turbulent flow by a mesh-free method. CMES-Comp Model Eng 2009;44:66–95.
[50] Courant R, Isaacson E, Rees M. On the solution of nonlinear hyperbolic differential equations by finite differences. Commun Pure Appl Math 1952;5:243–55.
[51] Lin H, Atluri SN. Meshless local Petrov Galerkin method (MLPG) for convection-diffusion problems. CMES-Comp Model Eng 2000;1:45–60.
[52] Malan AG, Lewis RW. An artificial compressibility CBS method for modelling heat transfer and fluid flow in heterogeneous porous materials. Int J Numer Meth Eng 2011;87:412–23.
[53] Arpino F, Massarotti N, Mauro A, Nithiarasu P. Artificial compressibility based CBS solutions for double diffusive natural convection in cavities. Int J Numer Method H 2013;23:205–25.
[54] Hong CP. Computer modelling of heat and fluid flow materials processing. Bristol: Institute of Physics Publishing; 2004.
[55] Kosec G, Depolli M, Rashkovska A, Trobec R. Super linear speedup in a local parallel meshless solution of thermo-fluid problems. Comput Struct 2013;11:016 (2014:10.1016/j.compstruc.).
[56] Kosec G, Zinterhof P. Local strong form meshless method on multiple Graphics Processing Units. CMES-Comp Model Eng 2013;91:377–96.
[57] Asai S, Sahara T, Muchi I. Theoretical analysis and model study of the formation of A-type segregation in ingots. Tetsu-To-Hagane/J Iron Steel Inst Japan 1977;63:1512–9.
[58] Kosec G, Šarler B. H-adaptive local radial basis function collocation meshless method. CMC-Comput Mater Con 2011;26:227–53.
[59] Kovačević I, Šarler B. Solution of a phase-field model for dissolution of primary particles in binary aluminum alloys by an r-adaptive mesh-free method. Mater Sci Eng 2005;A413-A414:423–8.
[60] Lorbiecka AZ, Šarler B. Simulation of dendritic growth with different orientation by using the point automata method. CMC-Comput Mater Con 2010;18:69–103.

Please cite this article as: Kosec G, Šarler B. Simulation of macrosegregation with mesosegregates in binary metallic casts by a meshless method. Eng. Anal. Boundary Elem. (2014), http://dx.doi.org/10.1016/j.enganabound.2014.01.016